



**HAL**  
open science

## Finite frequency external modulation in doubly diffusive convection

Olivier Sovran, Gérald Bardan, Abdelkader Mojtabi, Marie-Catherine Charrier-Mojtabi

► **To cite this version:**

Olivier Sovran, Gérald Bardan, Abdelkader Mojtabi, Marie-Catherine Charrier-Mojtabi. Finite frequency external modulation in doubly diffusive convection. *Numerical Heat Transfer, Part A Applications*, 2000, 37 (8), pp.877-896. 10.1080/10407780050045874 . hal-01958626

**HAL Id: hal-01958626**

**<https://hal.science/hal-01958626>**

Submitted on 18 Dec 2018

**HAL** is a multi-disciplinary open access archive for the deposit and dissemination of scientific research documents, whether they are published or not. The documents may come from teaching and research institutions in France or abroad, or from public or private research centers.

L'archive ouverte pluridisciplinaire **HAL**, est destinée au dépôt et à la diffusion de documents scientifiques de niveau recherche, publiés ou non, émanant des établissements d'enseignement et de recherche français ou étrangers, des laboratoires publics ou privés.



## Open Archive Toulouse Archive Ouverte

OATAO is an open access repository that collects the work of Toulouse researchers and makes it freely available over the web where possible

This is an author's version published in: <http://oatao.univ-toulouse.fr/20679>

**Official URL:**

<https://doi.org/10.1080/10407780050045874>

**To cite this version:**

Sovran, Olivier and Bardan, Gérald and Mojtabi, Abdelkader and Charrier-Mojtabi, Marie-Catherine Finite frequency external modulation in doubly diffusive convection. (2000) Numerical Heat Transfer, Part A: Applications, 37 (8). 877-896. ISSN 1040-7782

Any correspondence concerning this service should be sent to the repository administrator: [tech-oatao@listes-diff.inp-toulouse.fr](mailto:tech-oatao@listes-diff.inp-toulouse.fr)

# FINITE FREQUENCY EXTERNAL MODULATION IN DOUBLY DIFFUSIVE CONVECTION

**O. Sovran, G. Bardan, and A. Mojtabi**

*U.M.R. 5502 IMFT-CNRS-UPS, U.F.R. M.I.G., Université Paul Sabatier,  
31062 Toulouse Cedex, France*

**M.-C. Charrier-Mojtabi**

*LESETH, U.F.R. P.C. A., Université Paul Sabatier, 31062 Toulouse Cedex,  
France*

*Convective oscillations in porous and fluid media are studied numerically. A two-dimensional, square, differentially heated cavity, filled with a porous medium saturated by a binary fluid or simply by a binary fluid, is considered. This cavity is subjected to linear harmonic oscillations in the vertical direction. The formulation is based on the Darcy–Brinkman–Forchheimer–Boussinesq model. The time dependent Darcy–Brinkman–Forchheimer–Boussinesq equations are solved using a pseudo-spectral Legendre collocation method. The instantaneous and mean characteristics of the flows are studied and discussed. An intensification of the heat and mass transfers is observed at low frequency for sufficiently high vibration intensity. A comparison between the response to the imposed vibrations is made for Darcy numbers varying from  $Da = 10^{-7}$  to  $Da = 10$ .*

## INTRODUCTION

It is well known that one of the most interesting phenomena in binary mixtures is the arising of stratified flows responsible, particularly, for the formation of stratified structures in crystal growth in terrestrial or microgravity conditions. According to the existing knowledge, such flows arise as a result of instability of specific states in which the density variations are because of inhomogeneities in the temperature and concentration.

Fundamental studies on natural convection, within an enclosure subjected to intermittent heat flux from the side and filled with a fluid or with a fluid-saturated porous medium, have demonstrated the existence of convection resonance when the heat pulsation frequency approaches the natural flow frequency of the system. The case of periodic horizontal heating was studied by Antohe and Lage [1, 2] focusing on the natural resonance within a porous enclosure under a fixed amplitude of the heat flux. Their numerical simulations covered a wide range of input heat frequencies with the Darcy number ( $Da$ ) varying from  $10^{-2}$  to  $10^{-6}$  and

The authors gratefully acknowledge the C.I.N.E.S. (Centre Informatique National de l'Enseignement Supérieur, Montpellier, France) for its financial support.

## NOMENCLATURE

<p><math>a_*</math> effective thermal diffusivity (= <math>\lambda_* / (\rho c)_f</math>)</p> <p><math>b</math> displacement amplitude</p> <p><math>C</math> mass fraction</p> <p><math>Da</math> Darcy number (= <math>K/L^2</math>)</p> <p><math>D_*</math> effective solutal diffusivity</p> <p><math>f</math> frequency</p> <p><math>I</math> Forchheimer inertia parameter (= <math>1.75(Da/150\varepsilon^3)^{1/2}</math>)</p> <p><math>J</math> viscosity ratio (= <math>\mu_{eff}/\mu</math>)</p> <p><math>K</math> coefficient of permeability</p> <p><math>L</math> cavity side</p> <p><math>Le</math> Lewis number (= <math>a_*/D_*</math>)</p> <p><math>N</math> ratio of solutal and thermal buoyancy forces (= <math>(\beta_C \Delta C)/(\beta_T \Delta T)</math>)</p> <p><math>Nu</math> Nusselt number (= <math>\int_0^1 (u \cdot T - \partial T / \partial x)_{x=0.5} dz</math>)</p> <p><math>p</math> pressure</p> <p><math>Pr</math> Prandtl number (= <math>\nu/a_*</math>)</p> <p><math>R</math> ratio between the vibration and the gravity accelerations (= <math>b\hat{\omega}^2/g</math>)</p> <p><math>Ra_T</math> thermal Rayleigh number (= <math>(L^3 \beta_T \Delta T g) / \nu a_*</math>)</p>	<p><math>Ra_{TV}</math> thermovibrational Rayleigh number (= <math>(L^3 \beta_T \Delta T b \hat{\omega}^2) / \nu a_*</math>)</p> <p><math>Sh</math> Sherwood number (= <math>\int_0^1 (Le^{-u} \cdot C - \partial C / \partial x)_{x=0.5} dz</math>)</p> <p><math>t</math> time</p> <p><math>T</math> temperature</p> <p><math>U</math> filtration velocity vector</p> <p><math>x, y</math> coordinates</p> <p><math>\beta_C</math> coefficient of solutal expansion</p> <p><math>\beta_T</math> coefficient of thermal expansion</p> <p><math>\varepsilon</math> porosity</p> <p><math>\lambda_*</math> effective thermal conductivity</p> <p><math>\omega</math> angular frequency of vibration</p> <p><math>\rho</math> density</p> <p><math>\sigma</math> volumetric specific heat ratio (= <math>((\rho c)_* / (\rho c)_f)</math>)</p> <p><math>\nu</math> kinematic viscosity</p> <p style="text-align: center;"><b>Superscript</b></p> <p><math>n</math> time level</p> <p><math>\overline{(\cdot)}</math> mean function</p> <p><math>(\hat{\cdot})</math> dimensional value</p>
---------------------------------------------------------------------------------------------------------------------------------------------------------------------------------------------------------------------------------------------------------------------------------------------------------------------------------------------------------------------------------------------------------------------------------------------------------------------------------------------------------------------------------------------------------------------------------------------------------------------------------------------------------------------------------------------------------------------------------------------------------------------------------------------------------------------------------------------------------------------------------------------------------------------------------------------------------------------------------------------------------------------------------------------------------------------------------------------------------------------------------------------------------------------------------------------------------------------------------------------	-----------------------------------------------------------------------------------------------------------------------------------------------------------------------------------------------------------------------------------------------------------------------------------------------------------------------------------------------------------------------------------------------------------------------------------------------------------------------------------------------------------------------------------------------------------------------------------------------------------------------------------------------------------------------------------------------------------------------------------------------------------------------------------------------------------------------------------------------------------------------------------------------------------------------------------------------------------------------------------------------------------------------------------------------------------------------------------------------------

the Rayleigh number ( $Ra_T$ ) varying from  $10^6$  to  $10^{12}$ . Numerical simulations indicated that natural convection resonance was smoothed when the Prandtl number ( $Pr$ ) increased or decreased from the value  $Pr \sim 1$ . Their results indicated a reduced response of porous systems to oscillatory heating as the solid matrix became less permeable, the response being undetectable when  $Da \leq 10^{-6}$  within the range of parameters investigated. Concerning the effect of a mechanical vibrational field, our statement of the problem is close to that of Gershuni and Zhukhovitsky [3] and Yurkov [4] but is formulated for a two-component Darcy–Brinkman–Forchheimer model. In the case of a porous medium (with a Darcy model) the effect of vibrational convection exists, but only in the case of finite frequency (Khallouf, Gershuni, and Mojtabi [5]). Khallouf et al. found that this effect disappeared in the limiting case of high frequency and thought that this result was linked to the simplification they adopted using the Darcy model. Generally speaking, oscillatory phenomena are smoothed in a dissipative medium like a Darcy porous medium. In addition, oscillatory motions can appear in binary mixtures (Brand and Steinberg [6], Ourzazi and Bois [7]) as the result of convective instabilities.

## PROBLEM DESCRIPTION

We consider a two-dimensional square cavity of length  $L$ , filled with a nonreactive Boussinesq binary-fluid mixture saturated porous medium, subjected to lateral forcing by imposed temperature and concentration differences:  $T = T_1$ ,

$C = C_1$  at  $x = 0$ , and  $T = T_2, C = C_2$  at  $x = L$ , with  $\Delta T = T_1 - T_2 \geq 0, \Delta C = C_1 - C_2 \leq 0$ . The cavity is also subjected to vertical linear harmonic oscillations. The binary fluid has density  $\rho$  and kinematic viscosity  $\nu$ . The effective thermal conductivity of the porous medium is  $\lambda_*$ . The effective thermal diffusivity of the porous medium and the effective solutal diffusivity of the heavier component are, respectively,  $a_*$  and  $D_*$ . The porous medium is characterized by a porosity  $\varepsilon$ , a volumetric specific heat ratio  $\sigma$ , a permeability  $K$ , a viscosity ratio  $J$ , and a Forchheimer inertia coefficient  $I$ . Soret and Dufour effects will not be explicitly taken into account but can be incorporated easily into the treatment that follows by means of a transformation, including the Soret–Dufour equations into those used below (Knobloch [8]). We assume that within the range of temperature and concentration expected, the density varies linearly with the temperature and concentration:

$$\rho(T, C) = \rho_{\text{ref}}(1 - \beta_T(T - T_{\text{ref}}) - \beta_C(C - C_{\text{ref}})) \quad (1)$$

where  $\rho_{\text{ref}}$  is the density at temperature  $T_{\text{ref}} = T_2$  and mass fraction  $C_{\text{ref}} = C_1$ . In the following, we assume constant coefficients of thermal and solutal expansion  $\beta_T$  and  $\beta_C$ , respectively. For most fluids,  $\beta_T$  is positive. Assuming that  $C$  is the mass fraction of the heavier component,  $\beta_C$  is negative. To simulate convective flows both in fluid medium and in porous medium, we adopt a Darcy–Brinkman–Fochheimer model, written in the oscillating coordinate system. Thus the gravity field has to be replaced by the sum of the gravity and the vibrational acceleration,

$$g \rightarrow -gz - b\hat{\omega}^2 \sin(\hat{\omega}t)z \quad (2)$$

Let us define the frequency  $\hat{f}$  of vibration by the classical relation  $\hat{\omega} = 2\pi\hat{f}$ . The dimensionless temperature and concentration are taken to be  $(T - T_{\text{ref}})/\Delta T$  and  $(C - C_{\text{ref}})/\Delta C$ . Length, time, and velocity are nondimensionalized with  $L, \varepsilon L^2/a_*, a_*/L$ .

The resulting dimensionless equations are

$$\nabla \cdot U = 0 \quad (3)$$

$$\begin{aligned} \frac{\partial U}{\partial t} + (U \cdot \nabla)U = -\nabla P + \varepsilon^2 J \text{Pr} \nabla^2 U \\ + \varepsilon^2 \text{Ra}_T \text{Pr}(T - NC)(1 + R \sin(\omega t))z \end{aligned} \quad (4)$$

$$-\frac{I\varepsilon^2}{\text{Da}} \|U\|U - \frac{\text{Pr}\varepsilon^2}{\text{Da}} U$$

$$\frac{\sigma}{\varepsilon} \frac{\partial T}{\partial t} + (U \cdot \nabla)T = \nabla^2 T \quad (5)$$

$$\frac{\partial C}{\partial t} + (U \cdot \nabla)C = \frac{1}{\text{Le}} \nabla^2 C \quad (6)$$

where  $U = ux + wz$  is the dimensionless filtration velocity vector, and  $Ra_T$ ,  $R$ , respectively, are the thermal Ra and the ratio between the vibration and the gravity accelerations. The dimensionless frequency is defined by  $\omega = 2\pi f$  and parameter  $J$  in Eq. (4) accounts for the ratio of the effective viscosity of the fluid-saturated porous medium to the viscosity of the fluid. In the following, parameter  $J$  and the ratio  $\sigma/\varepsilon$  are taken equal to one; Pr is fixed and equal to 0.71. The expression for the Forchheimer inertia parameter  $I(= 1.75(Da/150\varepsilon^3)^{1/2})$ , shown in Eq. (4) follows the Ergun model [9]. In the dimensionless variables, the flow domain is  $(x, z) \in \Omega \equiv [0, 1] \times [0, 1]$ . The horizontal walls are taken to be insulating and across these two walls the normal mass flux is zero. No-slip boundary conditions are imposed along all boundaries. Thus

$$U = 0 \quad \text{along } \partial\Omega \quad (7)$$

$$T(x = 0, z) - 1 = T(x = 1, z) = C(x = 1, z) - 1 = C(x = 0, z) = 0 \quad (8)$$

$$\frac{\partial T}{\partial z}(x, z = 0, 1) = \frac{\partial C}{\partial z}(x, z = 0, 1) = 0 \quad (9)$$

We consider here the situation in which the buoyancy forces because of the thermal and solutal gradient contributions reinforce each other and are of equal intensity; i.e., the ratio of solutal and thermal buoyancy forces is equal to one:

$$N = \frac{\beta_C \Delta C}{\beta_T \Delta T} = 1 \quad (10)$$

## NUMERICAL METHOD

In this section we give a brief description of the numerical method employed and prove its accuracy when applied to a problem of natural convection in a differentially heated square cavity (our physical configuration) filled with a porous medium. The time dependent Eqs. (4), (5), (6) are discretized at time  $t^{n+1} = (n + 1)\Delta t$ , where  $n$  is the time level and  $\Delta t$  is the time step. The advection-diffusion energy, species conservation, and momentum equations are approximated semiimplicitly using an implicit second-order Euler backward scheme for linear terms and an Adams–Bashforth scheme for the nonlinear terms. Hence the semidiscrete equations read as follows:

$$\nabla^2 T^{n+1} - \frac{3\sigma}{\varepsilon 2\Delta t} T^{n+1} = -\frac{4T^n - T^{n-1}}{2\Delta t} + [2(U\nabla T)^n - (U\nabla T)^{n-1}] \quad (11)$$

$$\nabla^2 C^{n+1} - \frac{3\text{Le}}{2\Delta t} C^{n+1} = -\text{Le} \frac{4C^n - C^{n-1}}{2\Delta t} + \text{Le}[2(U\nabla C)^n - (U\nabla C)^{n-1}] \quad (12)$$

$$\left[ \nabla^2 - \left( \frac{3}{\varepsilon^2 \text{Pr} 2 \Delta t} + \frac{1}{Da} \right) \right] U^{n+1} = f(S^n, S^{n-1}) \quad (13)$$

$$(\nabla U)^{n+1} = 0 \quad (14)$$

A high accuracy spectral method, namely, the Legendre collocation method, with the Gauss–Lobatto zeros as collocation points, is used to solve the Helmholtz problem (11), (12) and the projection problem (13), (14). The well-known successive diagonalization technique is implemented to invert the corresponding operators. We must mention here that such a solver is direct and guarantees a spectral accuracy solution with free divergence for the  $U$  field on the whole domain, including the boundaries. The method, called projection diffusion, was developed by Azäiez, Ben Belgacem, Grundmann, and Khallouf [10] and solves the system in two steps:

$$U^* + \nabla P = S \quad \text{on } (\Omega) \quad (15)$$

$$\nabla U^* = 0 \quad \text{on } (\Omega) \quad (16)$$

$$U^* \cdot n = \left( \frac{\partial U}{\partial t} - \nabla^2 U \right) \cdot n \quad \text{along } (\partial\Omega) \quad (17)$$

which is called the projection step, where  $U^* = \partial U / \partial t - \nabla^2 U$  is the solenoidal part of  $S$  in Eq. (15). Next, the diffusion step is considered to determine the field  $U$  using a vectorial Helmholtz equation on  $U$ :

$$\frac{\partial U}{\partial t} - \nabla^2 U = U^* \quad \text{in } (\Omega) \quad (18)$$

$$U = f \quad \text{along } (\partial\Omega) \quad (19)$$

## RESULTS AND DISCUSSION

We define the instantaneous global Nusselt (Nu) and Sherwood (Sh) numbers:

$$\text{Nu}(t) = \int_0^1 \left( u \cdot T - \frac{\partial T}{\partial x} \right)_{x=0.5} dz \quad (20)$$

$$\text{Sh}(t) = \int_0^1 \left( \text{Le} u \cdot C - \frac{\partial C}{\partial x} \right)_{x=0.5} dz \quad (21)$$

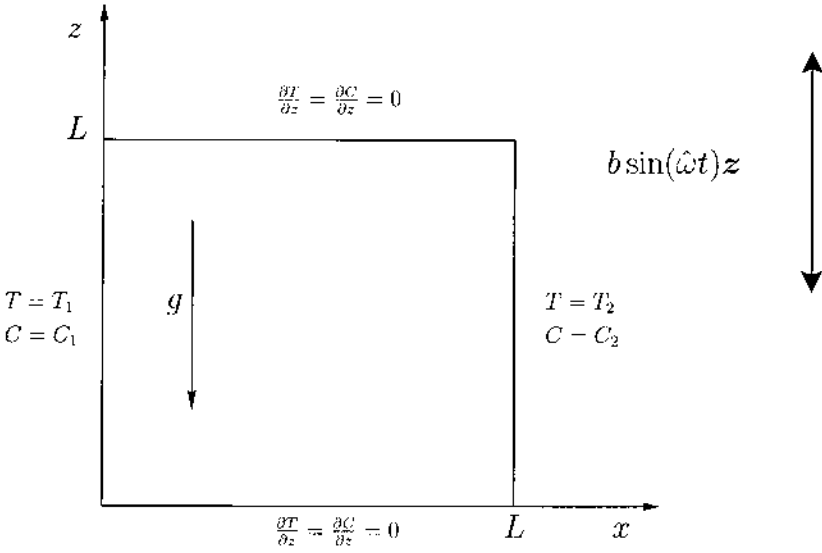


Figure 1. Cavity configuration.

The mean global Nu and Sh, respectively,  $\overline{\text{Nu}}$ ,  $\overline{\text{Sh}}$ , independent of the position  $x$  in the cavity, are defined by

$$\overline{\text{Nu}} = \frac{1}{\tau} \int_{t-\tau/2}^{t+\tau/2} \text{Nu}(s) ds \quad (22)$$

$$\overline{\text{Sh}} = \frac{1}{\tau} \int_{t-\tau/2}^{t+\tau/2} \text{Sh}(s) ds \quad (23)$$

with  $\tau = 1/f$ . The purpose is to examine the effect of the frequency vibration on the heat and mass transfer in the cavity. (See Figure 1.)

## Binary Fluid

The model (3)–(6) degenerates in the Navier–Stokes set of equations when  $\text{Da} > 10$ . Consequently, for  $\text{Da} > 10$  the  $\text{Da}$  variation does not affect the structure of the flow. This was confirmed by direct numerical simulations of Eqs. (3)–(6) with boundary conditions (7)–(9).

**Resonance in Amplitude  $R < 10$  and  $\text{Pr} = 0.71$ .** The vibrations do not affect the mean flow, but the amplitudes of all instantaneous fields (velocity, temperature, and concentration) depend on  $f$ . Figure 2 presents the amplitude  $A(\text{Sh})$  of the Sh versus the frequency  $f$  when the vibrational Ra is five times smaller than the thermal Ra ( $R = 1/5$ ,  $\text{Ra}_T = 10^5$ ,  $\text{Da} = 10$  and Le number

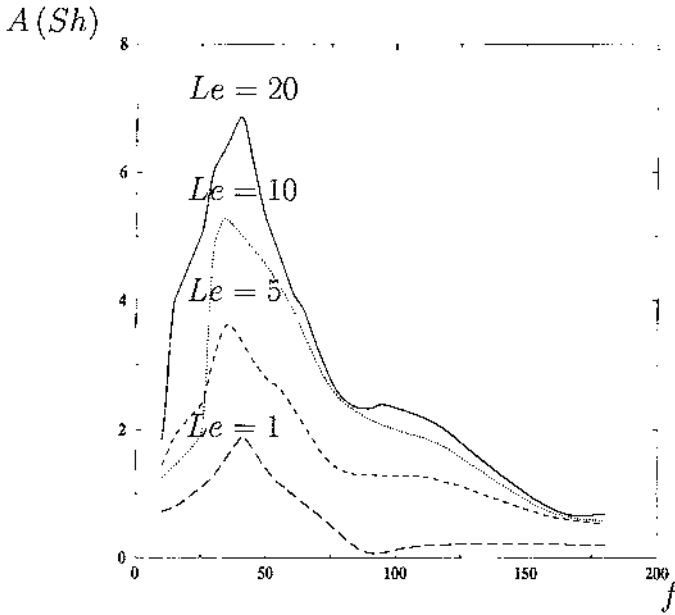


**Figure 2.** Amplitude of the instantaneous Sherwood number  $Sh$  versus the vibration frequency for different values of the Lewis number  $Le$ . Set of parameters:  $Da = 10$ ,  $Ra_r = 10^5$ ,  $Pr = 0.71$ , and  $R = 1/5$ . Resolution is  $33 \times 33$ .

varying from 1 to 20). A *resonance phenomenon* is observed for  $f \sim 50$  for all values of  $Le$ . The fluctuation of the  $Sh$  is linked with the  $Le$ , and an increasing resonance intensity is observed when the  $Le$  value increases. When  $Le$  is increased, the thermal inhomogeneities are reduced quickly (in comparison with the solutal ones) and the system allows larger amplitudes in the time variation of the mass flux. For large values of  $f$ , the Fourier transforms in frequency (Figure 3) show that  $Sh$  (like the velocities or the  $Nu$ ) has a sinusoidal time evolution with a frequency corresponding to the imposed one,  $f_{out} = f$ . For  $f > 120$ , the assumptions of the averaged equations model are valid and available for computations (see Gershuni and Zhukhovitsky [11] and Gershuni and Lyubimov [12]). In the range of  $f < 120$ , a superharmonic  $f_{out} = 2f$  because of the nonlinear effects of vibrations occurs, but its intensity remains very small. These superharmonics intensify with increasing  $R$  and lead to the intensification of the heat and mass transfer in the cavity.

**Vibrational Mean Flow  $R > 10$  and  $Pr = 0.71$ .** In this paragraph, acceleration because of the vibrational field is more than  $10g$ . In Figure 4 is plotted the mean  $Nu$  value  $\overline{Nu}$  varying with the frequency  $f$  for  $R = 0, 10, \text{ and } 100$ ;  $Ra_r = 10^4$ ;  $Da = 10$ ; and  $Le = 1$ . The heat transfer is enhanced whenever the values of  $f$  and the heat flux increases with  $R$ . Effects of vibrations are singularly different at low or high frequencies.

# Intensity

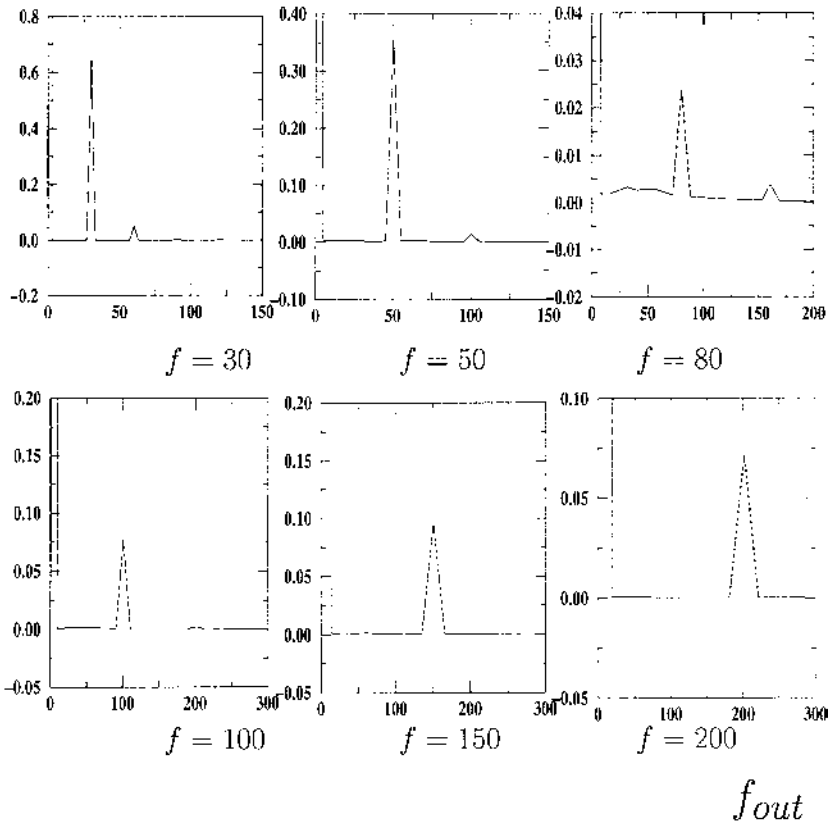


**Figure 3.** Fourier transform into frequency of the instantaneous Sherwood number for different vibration frequencies  $f$ . Set of parameters:  $Le = 10$ ,  $Pr = 0.71$ ,  $Da = 10$ ,  $Ra_r = 10^5$ , and  $R = 1/5$ . Resolution is  $33 \times 33$ .

Within the high frequencies, all the mean fields become *independent* of  $f$ . The ellipsoidal phase diagram in the  $u - w$  plane plotted for an imposed vibration of  $f = 800$  (inset in Figure 4) is typical of a pure sinusoidal signal. This diagram is completed by the Fourier transform of  $Nu$ . Only the frequency  $f$  of the source is transmitted by the system.

The nonlinear effects of the vibrational field appear for low frequencies via many superharmonics in the response of the system. These superharmonics could have an energy larger than the one at the source frequency  $f$ . The inset of Figure 4 shows the Fourier diagram of  $Nu$  for  $f = 50$ . The major frequency in the spectrum of  $Nu$  is  $f_{out} = 2f$ .

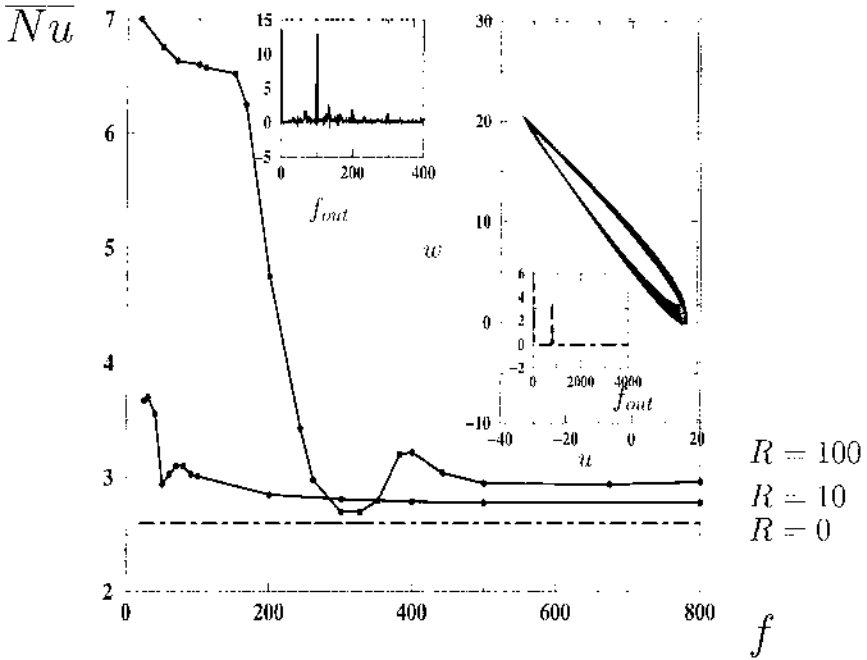


**Figure 4.** Variation of the mean Nusselt number  $\overline{Nu}$  with the frequency  $f$  for  $R = 0$  (dashed line),  $R = 10$  and  $R = 100$ ,  $Pr = 0.71$ ,  $Ra_T = 10^4$ ,  $Da = 10$ , and  $Le = 1$  (solid lines). Inset for  $R = 100$ : upper left, Fourier transform into frequency of the Nusselt number for  $f = 50$  and, right, parametric velocities diagram in the  $u(x = z = 0.25) - w(x = z = 0.25)$  plane and the Fourier transform into frequency of the Nusselt number for  $f = 800$ . Resolution is  $33 \times 33$ .

Figure 5 presents the mean streamfunctions and the mean isotherms for various frequencies  $f$  when  $R = 100$ . At low frequencies ( $f < 120$ ), the heat transfer is enhanced by a thermal boundary layer regime. The flow consists of a four-vortex structure that is characteristic of the vibrational convection mechanism. When the vibration frequency is increased, a thermovibrational flow appears. The interaction between natural (one cell) and vibrational (four cells) convection leads to considerable modifications of the flow structures and isotherms. The recirculations disappear progressively as  $f$  increases, and the flow structure tends to a main cell, which occupies the entire cavity. Concurrently the isotherms become perpendicular to the axis of vibration, that is, horizontal in the core region, which corresponds to the well-known natural or thermosolutal structure or both. This behavior has been observed by Lizée [13].

### Binary-Fluid Saturated Porous Medium

In this part we study the flow response for  $Da$  lower than or equal to  $10^{-4}$ . The characteristics of instantaneous and mean fields greatly change with the ratio  $R$ . First, these characteristics are listed and compared with the binary fluid cases

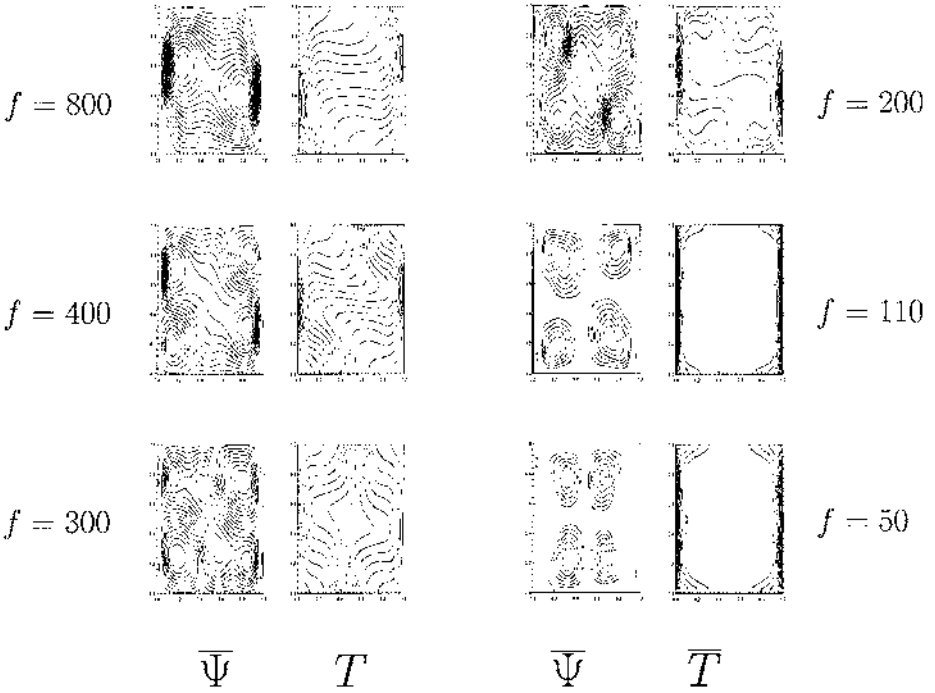


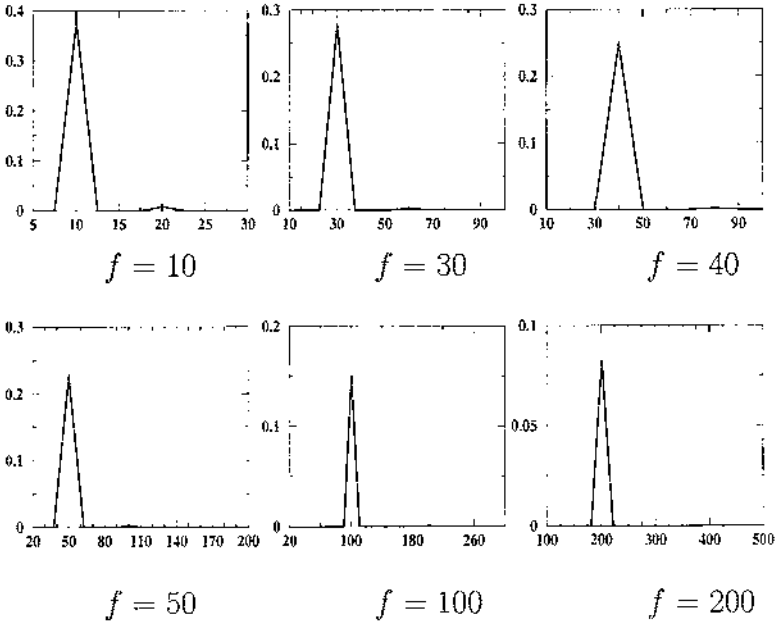
**Figure 5.** Mean streamlines and mean isotherms for different frequencies  $f$ . Set of parameters:  $Ra_T = 10^4$ ,  $R = 100$ ,  $Da = 10$ ,  $Pr = 0.71$ , and  $Le = 1$ . For increasing  $f$ , isotherms become perpendicular to the axis of vibration. Resolution is  $33 \times 33$ .

for a fixed value of the  $Da$  ( $Da = 10^{-4}$ ) and then generalized to lower  $Da$  in the last part ( $10^{-7} \leq Da \leq 10^{-4}$ ). To enable comparison between the Darcy–Brinkman–Forchheimer model and the Darcy model, we define a modified  $Ra$   $Ra_D$  as the product  $Ra_T Da$ . This number exactly corresponds to the thermal  $Ra$  generally defined for the Darcy model.

**Resonance in Amplitude  $R < 10$ ,  $Ra_D = 100$ ,  $Pr = 0.71$ , and  $Da = 10^{-4}$ .** In the case  $R < 10$ , the mean fields are almost independent of the frequency as indicated in Figure 8. (Case  $R = 1$ ; for low frequencies we observe a very low relative variation of the mean  $Nu$ .) In Figure 6 the diagram of the Fourier transform of the  $Sh$  is plotted for  $R = 1/5$  and  $Le = 1$ . A very small nonlinear effect is observed for  $f \leq 50$  with the presence of a superharmonic  $f_{out} = 2f$ . It disappears totally for sufficiently high frequencies. We observe a similar behavior to that in a binary fluid (see Figure 3). This result is extended to  $Le$  varying from 1 to 20.

However, a *resonance in amplitude* for instantaneous heat and mass transfers is obtained for  $f \sim 40$  (in the case  $R = 1/5$ ) and for all the  $Le$  values studied. In Figure 7 the variation of these amplitudes with frequency for  $R = 1/5$  and  $Le$

# Intensity



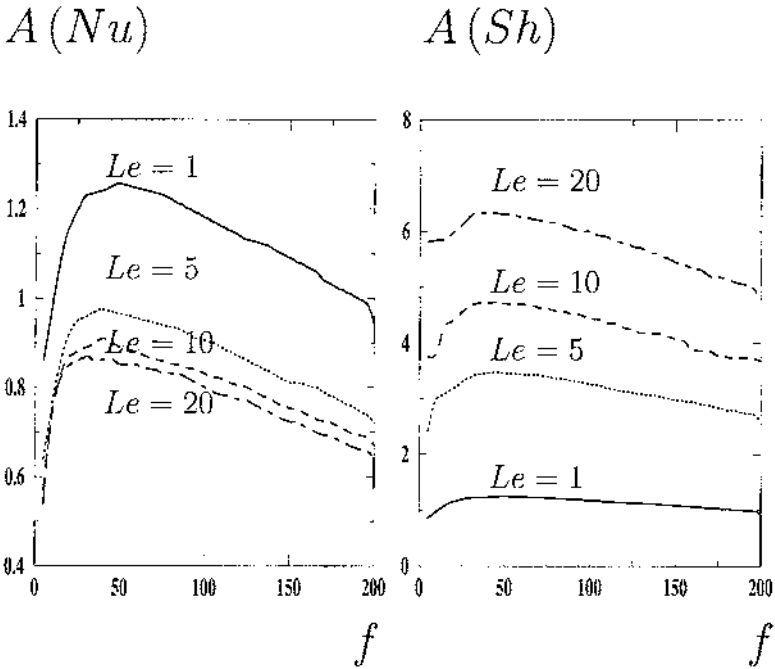
$f_{out}$

**Figure 6.** Fourier transforms into frequency of instantaneous Sherwood numbers for different vibration frequencies  $f$ . Set of parameters:  $Da = 10^{-4}$ ,  $Pr = 0.71$ ,  $Le = 1$ ,  $Ra_D = 100$ , and  $R = 1/5$ . Resolution is  $33 \times 33$ .

varying from 1 to 20 illustrates this result. The resonance frequency does not vary with the  $Le$  in the range of  $Le$  studied.

These resonance amplitude values are smoothed, in comparison with the binary-fluid case for the instantaneous  $Nu$  and  $Sh$ . The dissipative structure of the porous medium easily can explain this effect. All these results apply for  $R = 1$ . Behaviors of the main characteristics have been studied but not plotted.

This *resonance phenomenon* has been observed already by Antohe and Lage [1, 2]. Their system, a fluid or a fluid-saturated porous medium, was subjected to a constant temperature on  $x = 0$  and to a periodical heat flux on  $x = 1$ . The horizontal walls were insulated and no-slip boundary conditions applied for the velocity. Using the Darcy–Brinkman–Forchheimer model under the Boussinesq approximation, they obtained a resonance frequency. A scaling analysis coupled with numerical results demonstrated the equality between the period of recirculation into the cavity and the resonance’s period.

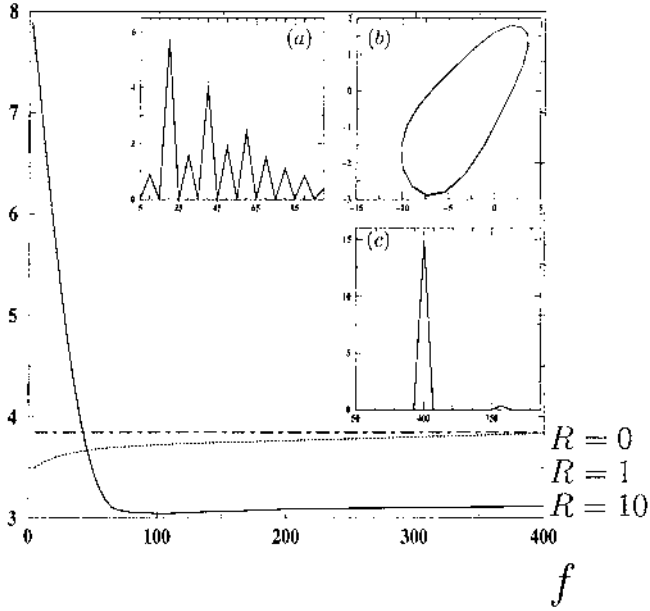


**Figure 7.** Amplitudes of global instantaneous Nusselt and Sherwood numbers, respectively,  $A(Nu)$  and  $A(Sh)$ , versus the frequency  $f$  for different Lewis numbers,  $Le = 20$  (dotted-dashed lines),  $Le = 10$  (dotted lines),  $Le = 5$  (dashed lines), and  $Le = 1$  (solid lines). Set of parameters:  $Da = 10^{-4}$ ,  $Ra_D = 100$ ,  $Pr = 0.71$ , and  $R = 1/5$ . Resolution is  $33 \times 33$ .

**Vibrational Mean Flow  $R > 10$ ,  $Pr = 0.71$ , and  $Da = 10^{-4}$ .** For the case  $R > 10$ , at low frequencies, the mean  $Nu$  and  $Sh$  greatly depend on the frequency, as observed in binary fluids.

Figure 8 compares the cases  $R = 0$ ,  $R = 1$ , and  $R = 10$  for  $Ra_D = 100$  and  $Le = 1$ . For  $R = 1$ , the heat transfer increases slightly with  $f$  and asymptotically tends to the case  $R = 0$  (i.e., no vibration) for  $f \geq 40$ , and reaches a constant value for  $f \geq 300$ . A major superharmonic  $f_{out} = 2f$  and many superharmonics for low frequencies reveal the presence of nonlinear effects, whereas *no mean field varies with frequency* for  $f \geq 300$ . Only the frequency of the source is transmitted by the system (Figure 8c) for  $f = 400$ . The typical ellipsoidal signal of the phase diagram in the  $u - w$  plane (Figure 8b) is observed for  $f = 400$ .

Figure 9 shows the variation with frequency of mean streamfunction and isotherm fields for  $Ra_D = 100$ ,  $R = 10$ , and  $Le = 1$ . A thermal boundary layer regime is observed for low frequencies and, as  $f$  increases, isotherms become perpendicular to the axis of vibration in the core region. Concurrently, for increasing frequencies, the streamfunctions tend to the natural thermosolutal convection with a main cell occupying the entire cavity.

$$\overline{Nu}$$


**Figure 8.** Variation of the mean Nusselt number  $\overline{Nu}$  with the frequency  $f$  for  $R = 0$  (dotted-dashed lines),  $R = 1$  and  $R = 10$  (solid lines). Set of parameters:  $Ra_D = 100$ ,  $Da = 10^{-4}$ ,  $Pr = 0.71$ , and  $Le = 1$ . Inset for  $R = 10$ : (a) Fourier transform into frequency of the instantaneous Nusselt number for  $f = 10$ ; (b) phase diagram in the  $u(x = z = 0.5) - w(x = z = 0.5)$  plane; and (c) Fourier transform into frequency of the instantaneous Nusselt number for  $f = 400$ . Resolution is  $33 \times 33$ .

In Figure 10, Fourier transform of the instantaneous  $Nu$  into frequency are presented for different imposed frequencies, for  $Ra_D = 100$ ,  $R = 10$ , and  $Le = 1$ . For low frequencies, the superharmonic  $f_{out} = 2f$ , with many other superharmonics, characterizes the nonlinear effects. Their intensity decreases with increasing  $f$  and totally disappears for high frequencies.

Figure 11 shows the variation of  $Nu$  and  $Sh$  Fourier transform with  $Le$  for  $f = 10$ ,  $Ra_D = 10$ , and  $R = 10$ . We can define a ratio  $r_f$  between the intensity for  $f_{out} = 2f$  and the intensity for  $f_{out} = f$ . For  $Sh$ , it is shown that this ratio decreases from 3 for  $Le = 1$  to 0.2 for  $Le = 20$ , whereas  $r_f$  stays constant and equal to 3 for the heat transfer as  $Le$  varies. Consequently, the mean mass transfer becomes independent of the frequency faster than the mean heat transfer. This result is confirmed by the variation with  $f$  of the  $\overline{Nu}$  and  $\overline{Sh}$  in Figure 12 for  $Ra_D = 10$  and  $R = 10$ , plotted for different  $Le$ .  $\overline{Sh}$  is constant for  $f \geq 30$ , whereas  $\overline{Nu}$  ceases to vary with frequency for  $f \geq 120$ .

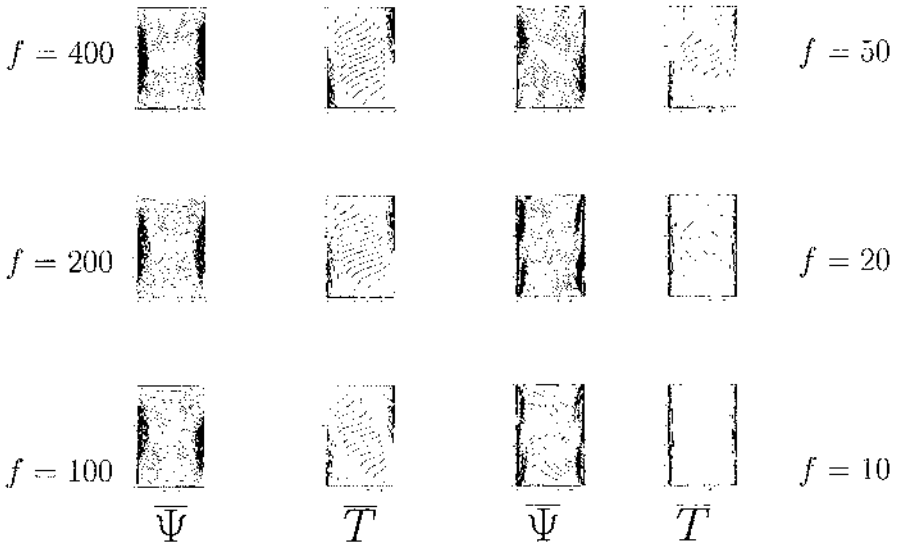


**Figure 9.** Mean streamlines and isotherms for different frequencies  $f$ . Set of parameters:  $Ra_D = 100$ ,  $R = 10$ ,  $Da = 10^{-4}$ ,  $Pr = 0.71$ , and  $Le = 1$ . Resolution is  $33 \times 33$ .

For the whole range of parameters studied, the variation of mean transfers is characterized by Fourier transforms of instantaneous Nu and Sh into frequency. It is shown that maximum transfers correspond to the presence of a large superharmonic intensity at  $f_{out} = 2f$  for low frequencies, and that mean fields become constant with  $f$  when superharmonics vanish for high frequencies.

**Variation of the Nusselt Number with the Darcy Number for  $Ra_D = 10$ ,  $Pr = 0.71$ .** Such a mathematical formulation enables us to make a study for different Da. The influence of the Da is compared numerically in Figure 13. The variation with frequency of the mean Nu is plotted for  $Le = 1$ ,  $R = 10$ , and Da varying from  $10^{-7}$  to  $10^{-4}$ . For all imposed Da, mean heat transfers decrease with the frequency and tend to a constant value for  $f \geq 150$ . This behavior is studied more precisely in Figure 14 for  $Da = 10^{-6}$ ,  $Le = 1$ , and different values of  $R$ . Maximum transfers correspond to the presence of high superharmonic intensity at  $f_{out} = 2f$  for low frequencies (see Figure 14a), and mean fields do not vary with the frequency for  $f \geq 200$ . This is confirmed by the plot in Figure 14b of the instantaneous Nu Fourier transform into frequency for  $f = 400$ . The intensity of the superharmonic at  $f_{out} = 2f$  is negligible and insures constant mean fields.

Khallouf et al. [5] studied the problem for a pure fluid using the Darcy model. For  $Ra_T = 200$  (corresponding to  $Ra_D$  as defined here) and  $R = 5/2$ , the study showed the mean isotherm field becoming perpendicular to the vibrational axis in the core region for increasing  $f$  and enhanced heat transfer for low frequencies with a thermal boundary layer regime. It is shown also that as  $f$  increases all the mean fields tend to the well-known thermal natural convection.

## Intensity

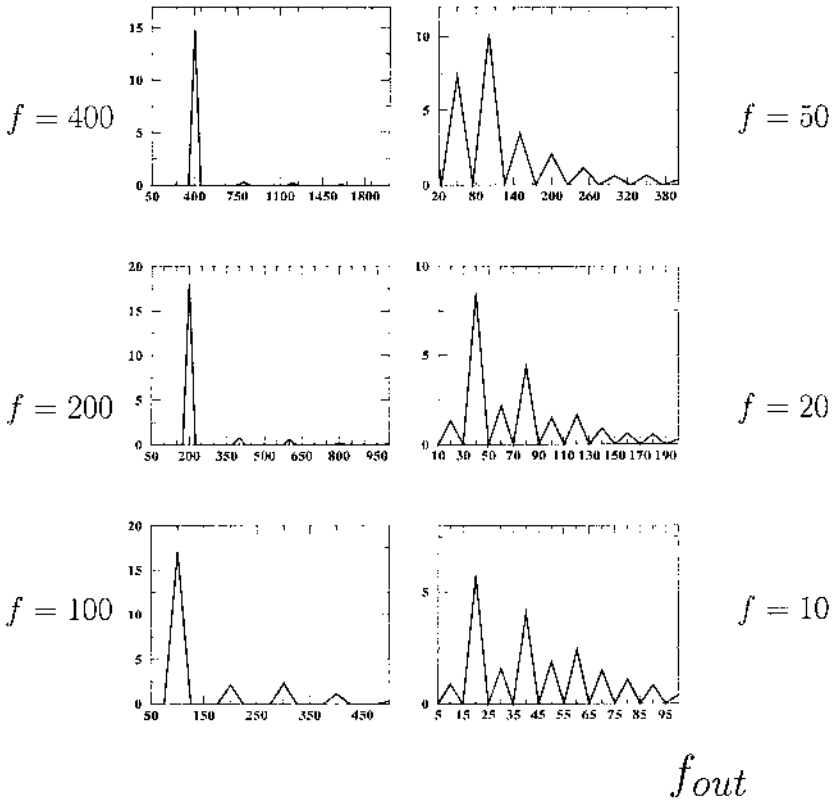


**Figure 10.** Fourier transform into frequency of the instantaneous Nusselt number for different vibration frequencies  $f$ . Set of parameters:  $Ra_D = 100$ ,  $R = 10$ ,  $Da = 10^{-4}$ ,  $Pr = 0.71$ , and  $Le = 1$ . A superharmonic  $f_{out} = 2f$  is observed at low frequency and disappears progressively with increasing  $f$ . Resolution is  $33 \times 33$ .

## CONCLUSION

Convective oscillations have been considered both in binary fluids and in a porous medium saturated with a binary fluid in a square, differentially heated cavity subjected to vertical oscillations. The instantaneous and mean characteristics of the flows have been studied. In the limiting case of *high frequencies*, effects of vibrational convection disappear in binary fluids and fluid-saturated porous media. Consequently, an *averaged* equations version of the Darcy–Brinkman–Forchheimer model is valid within the range of sufficiently high frequencies.

When the ratio  $R = Ra_{TV}/Ra_T$  is low ( $R \leq 10$ ), the mean flow is not affected by the vibrations, but a resonance of the amplitude of instantaneous  $Nu$  and  $Sh$  is observed. The intensity of the resonance is smoothed in the porous

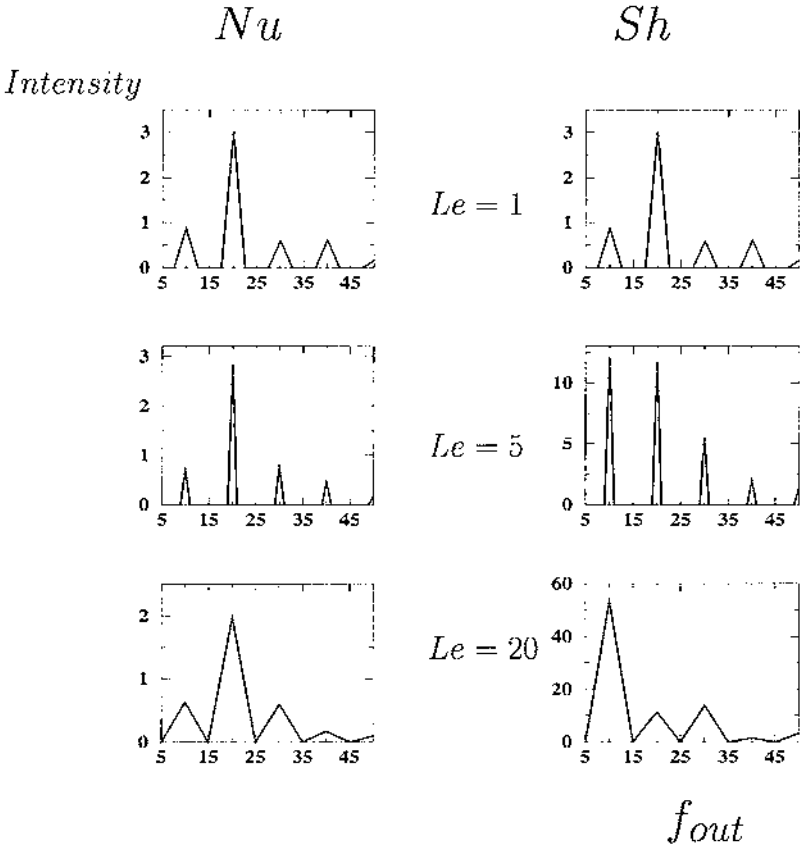
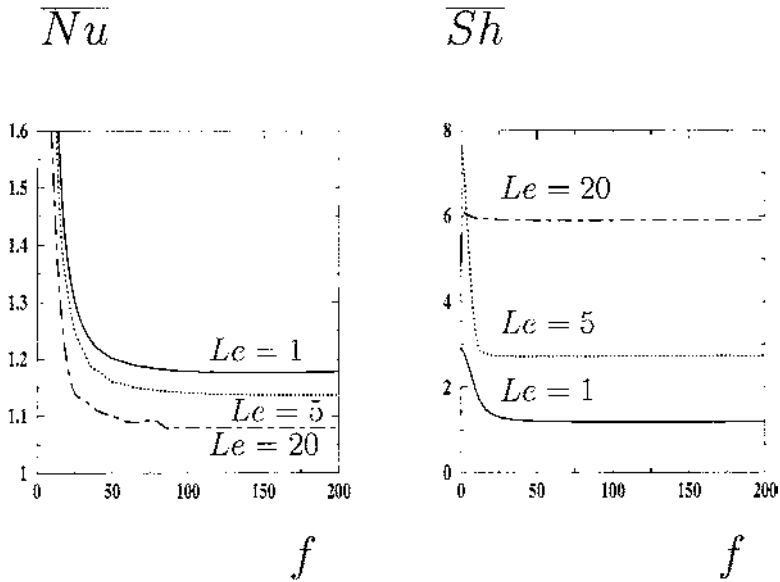


**Figure 11.** Fourier transforms of the global instantaneous Nusselt and Sherwood numbers for different Lewis numbers. Set of parameters:  $Ra_D = 10$ ,  $R = 10$ ,  $Da = 10^{-4}$ ,  $Pr = 0.71$ , and  $f = 10$ . For the Sherwood number, the ratio between the intensity at  $f_{out} = 2f$  and that at  $f_{out} = f$  decrease with the Lewis number. Resolution is  $33 \times 33$ .

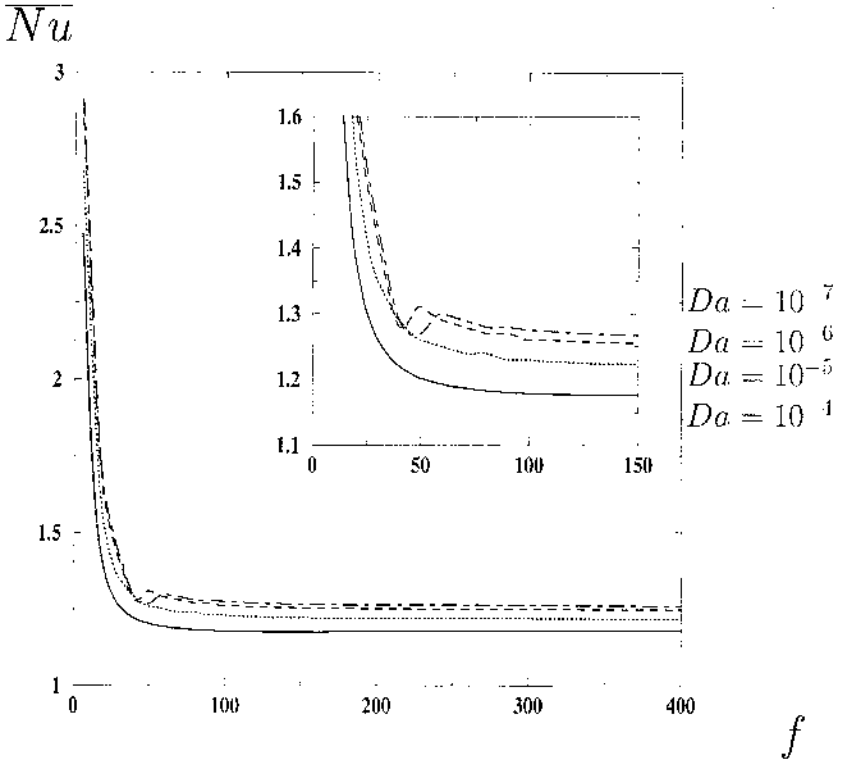
medium compared with the fluid one. The resonance frequency is independent of the  $Le$  in the range of parameters investigated.

When the ratio  $R$  is high enough ( $R \geq 10$ ), it is shown that significant modifications of the mean flows and of mean heat and mass transfers are obtained in the range of low frequencies, leading to an intensification of heat and mass transfers in the cavity. Vibrational effects decrease when the frequency increases, whereas the basic natural or thermosolutal convection flow or both is established in the limiting case of infinite frequencies.

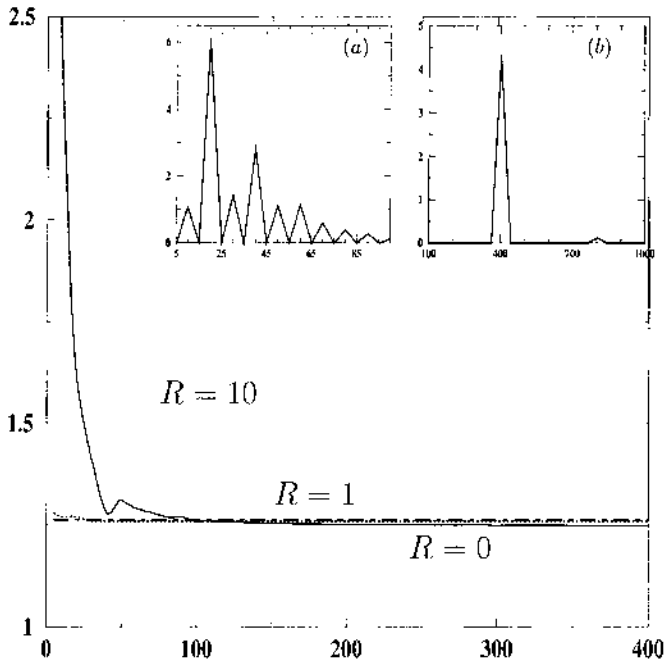
The results are of great importance for space experiments, in which the g-jitter produces accelerations at least 10 times larger than the residual gravity.



**Figure 12.** Variation of the mean Nusselt  $\overline{Nu}$  and Sherwood  $\overline{Sh}$  numbers with the frequency  $f$  for different Lewis numbers,  $Le = 20$  (dotted-dashed lines),  $Le = 5$  (dotted lines), and  $Le = 1$  (solid lines). Set of parameters:  $Ra_D = 10$ ,  $R = 10$ ,  $Pr = 0.71$ , and  $Da = 10^{-4}$ . For increasing  $Le$ , the  $\overline{Nu}$  decreases while the  $\overline{Sh}$  increases. Resolution is  $33 \times 33$ .



**Figure 13.** Variation of the mean Nusselt number  $\overline{Nu}$  with the frequency  $f$  for different Darcy numbers,  $Da = 10^{-4}$  (solid lines),  $Da = 10^{-5}$  (dotted line),  $Da = 10^{-6}$  (dashed lines), and  $Da = 10^{-7}$  (dotted-dashed lines). Set of parameters:  $Ra_D = 10$ ,  $R = 10$ ,  $Pr = 0.71$ , and  $Le = 1$ . Resolution is  $43 \times 43$ .

$\overline{Nu}$  $f$ 

**Figure 14.** Variation of the mean Nusselt number  $\overline{Nu}$  with the frequency  $f$  for  $R = 0$ ,  $R = 1$ , and  $R = 10$ . Set of parameters:  $Ra_D = 10$ ,  $Da = 10^{-6}$ ,  $Pr = 0.71$ , and  $Le = 1$ . Inset for  $R = 10$ : (a) Fourier transform into frequency of the Nusselt number for  $f = 10$ , and (b) Fourier transform into frequency of the Nusselt number for  $f = 400$ . Resolution is  $43 \times 43$ .

## REFERENCES

1. B. V. Antohe and J. L. Lage, Amplitude Effect on Convection Induced by Time-Periodic Horizontal Heating, *Int. J. Mass. Transfer.*, vol. 39, no. 6, pp. 1121–1133, 1996.
2. B. V. Antohe and J. L. Lage, The Prandtl Number Effect on the Optimum Heating Frequency of an Enclosure Filled With Fluid or With a Saturated Porous Medium, *Int. J. Mass. Transfer.*, vol. 40, no. 6, pp. 1313–1323, 1997.
3. G. Z. Gershuni and E. M. Zhukhovitsky, Convective Oscillations in a Closed Cavity in Modulated Gravity Field, *Convective Flows*, pp. 73–80, Perm, 1979.
4. Y. S. Yurkov, Vibrational Convection in Square Cavity in Weightlessness (Finite Frequencies), *Convective Flows*, pp. 98–103, Perm, 1981.
5. H. Khallouf, G. Z. Gershuni, and A. Mojtabi, Numerical Study of Two-Dimensional Thermovibrational Convection in Rectangular Cavities, *Numer. Heat Transfer, Part A*, pp. 297–305, 1995.
6. H. R. Brand and V. Steinberg, Convective Instabilities in Binary Mixture in a Porous Medium, *Physica*, vol. 119A, pp. 327–338, 1983.
7. M. N. Ourzazi and P. A. Bois, Convective Instability in of Fluid Mixture in a Porous Medium With Time-Dependent Temperature Gradient, *Eur. J. Mech. B/Fluids*, vol. 13, no. 3, pp. 275–298, 1994.
8. E. Knobloch, Convection in Binary Fluids, *Phys. Fluids*, vol. 23, pp. 1918–1920, 1980.
9. S. Ergun, Fluid Flows Through Packed Columns, *Chemicals Engrg. Progress*, no. 48, pp. 89–94, 1978.
10. M. Azäiez, F. Ben Belgacem, M. Grundmann, and H. Khallouf, Staggered Grids Hybrid-Dual Spectral Element Method for Second Order Elliptic Problems, *Comput. Meth. Appl. Mech. Engrg.*, vol. 166, no. 3–4, pp. 183–189, 1998.
11. G. Z. Gershuni and E. M. Zhukhovitsky, On Free Thermal Convection in Vibrational Field in Weightlessness, *Dokl. Akad. Nauk SSSR*, vol. 294, pp. 580–584, 1979.
12. G. Z. Gershuni and D. U. Lyubimov, *Thermal Vibrational Convection*, Wiley, New York, 1998.
13. A. Lizée, Contribution à la convection vibrationnelle Contrôle actif de la convection naturelle, Ph.D. thesis, University of Aix Marseille, 1995.
14. M. Azaïez, C. Bernardi, and M. Grundmann, Spectral Method Applied to Porous Media, *East-West J. Numer. Math.*, vol. 2, pp. 91–105, 1994.
15. P. Chang, Heat Transfer in Geothermal Systems, *Advances in Heat Transfer*, no. 14, pp. 1–105, 1978.
16. C. Canuto, M. Y. Hussaini, A. Quartaroni, and T. A. Zang, *Spectral Methods in Fluid Dynamics*, Springer-Verlag, New York, 1987.
17. H. Khallouf, Simulation numérique de la convection thermo-vibrationnelle par une méthode spectrale, Ph.D. thesis, University of Paul Sabatier Toulouse III, 1995.